Letters

Interleaved Boundary Conduction Mode Versus Continous Conduction Mode Magnetic Volume Comparison in Power Converters

Pablo Antoszczuk, Rogelio Garcia Retegui, and Gustavo Uicich, *Senior Member, IEEE*

***Abstract*—Power converters operating in boundary conduction mode (BCM) can benefit from an efficiency increase compared to continuous conduction mode (CCM) based on the soft-switching transitions at turn-ON and/or turn-OFF. However, for a given average inductor current, the RMS current in BCM converters becomes larger than in CCM converters, leading to an increase in conduction losses. Interleaving smaller BCM power converters overcome this drawback by reducing the total ripple current amplitude at the expense of an increase in complexity and in magnetic parts count. Nevertheless, as the magnetic devices are among the largest components in power converters, it is convenient to find the design conditions under which BCM or CCM could yield the smaller net volume. This paper proposes a method to estimate the volume ratio for magnetic parts, between single-phase CCM and multiple interleaved BCM power converters as a function of the number of phases, inductor loss, and switching frequency. The results obtained can be applied to boost, forward, and flyback dc-to-dc topologies.**

***Index Terms*—Boundary conduction mode (BCM), continuous conduction mode (CCM), inductor design, interleaved power converters, photovoltaic (PV) converters, power factor correction (PFC).**

I. Introduction

SWITCHING power converters have become widely used in renewable energy dc/dc converters and power factor correction (PFC) front ends [1]–[3]. The efficiency achieved in these applications can be improved by having the converter operate in boundary conduction mode (BCM), which reduces most of the reverse recovery and hard switching losses found in continuous conduction mode (CCM) [4]. However, as the peak-to-peak inductor current ripple in BCM is twice as much the average inductor current, the increase in conduction losses and in differential mode noise, limit the power throughput typically to a few hundreds watts [1]. These issues can be mitigated by interleaving N power converters, such that the total current is divided among the N constituent phases. Hence, the amplitude of the inductor ripple current becomes smaller with a frequency N-times higher the individual switching frequency, therefore reducing the requirements and losses in the differential mode filter [5].

Besides the efficiency advantage obtained with N-BCM the N-phase interleaved BCM converters over 1-CCM—the single-phase CCM converter—by trading off complexity, it is also relevant to assess the volume related to both topologies as it impacts the overall size and cost [6]. Interleaved power converters allow to reduce size of semiconductor devices and filter capacitors [7]–[9]. However, as the magnetic devices are among the largest components in power converters [10]–[12], it is necessary to determine how the total volume associated to the N-interleaved BCM inductors compares to the volume of a single CCM inductor for a constant load power converter.

This paper presents a method to estimate the total inductor volume ratio between 1-CCM and N-BCM interleaved converters, as a function of N, the number of phases, taking into consideration winding and core losses.

II. Proposed Method

The volume of an inductor can be estimated using the area product A_p criteria, which is associated to its energy-handling capability [13]. The area product, defined as the product between the core cross-sectional surface A_c and the window area W_a, is related to the electrical characteristics as:

$$A_p = A_c W_a = \frac{L\,\hat{i_L}\,I_{L_{\mathrm{RMS}}}}{J B_{\max} K_w} \tag{1}$$

where L is the inductor value, $\hat{i_L}$ is its peak current, $I_{L_{\mathrm{RMS}}}$ is the RMS inductor current, J is the winding current density, $B_{\max}$ is the maximum magnetic field density, and $K_w < 1$ is the copper fill factor. Notice (1) provides an estimate based on maximum flux swing related to $\hat{i_L}$.

As A_p has linear dimensions raised to the fourth power, inductor volume can be estimated as follows [13]:

$$\mathrm{Vol} = {A_p}^{(3/4)}. \tag{2}$$

Hence, the ratio between 1-CCM inductor volume $\mathrm{Vol}_{\mathrm{CCM}}$, and the N-BCM counterpart $\mathrm{Vol}_{\mathrm{BCM}(N)} = N\mathrm{Vol}_{\mathrm{BCM}(1)}$, can be obtained by calculating the area product for each case.

Fig. 1 shows the inductor current for 1-CCM and N-BCM operation. As previously stated, in 1-CCM converter the load current is provided by a single converter, being $\overline{i_{L_{\mathrm{CCM}}}}$ the

Manuscript received March 03, 2016; revised April 05, 2016 and April 14, 2016; accepted April 19, 2016. Date of publication April 27, 2016; date of current version July 08, 2016. This work was supported in part by the Universidad Nacional de Mar del Plata, Argentina, the Consejo Nacional de Investigaciones Cientficas y Tecnolgicas project PIP 0210, Argentina, by the Ministerio de Ciencia, Tecnologa e Innovacin Productiva, Argentina, and by the Agencia Nacional de Promocin Cientfica y Tecnolgica, Argentina.

The authors are with the Instituto de Investigaciones Cientficas y Tecnolgicas en Electrnica, Consejo Nacional de Investigaciones Cientficas y Tecnolgicas, Facultad de Ingeniera, Universidad Nacional de Mar del Plata, Mar del Plata 7600, Argentina (e-mail: pablo_ant@fi.mdp.edu.ar; rgarcia@fi.mdp.edu.ar; guicich@fi.mdp.edu.ar).

Digital Object Identifier 10.1109/TPEL.2016.2558469

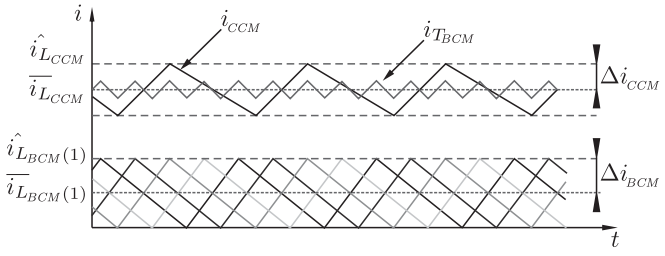

Fig. 1. DC/DC inductor current. CCM and BCM operation.

inductor mean current, with a ripple Δi_{CCM}. On the other hand, each BCM converter has Δi_{BCM} current ripple, equal to its mean value, $\overline{i_{L_{\mathrm{BCM}(1)}}}$. Notice each BCM mean current is N times smaller than 1-CCM average current.

Introducing k, the CCM ripple factor, as the ratio between mean and peak inductor current

$$k \triangleq \frac{\overline{i_{L_{\mathrm{CCM}}}}}{\hat{i}_{L_{\mathrm{CCM}}}} \leq 1. \tag{3}$$

The following relationships can be established:

$$\Delta i_{\mathrm{CCM}} = (1-k)\,\hat{i}_{L_{\mathrm{CCM}}} = \frac{1-k}{k}\,\overline{i_{L_{\mathrm{CCM}}}}. \tag{4}$$

Additionally, individual BCM peak and mean values can be related to CCM values as

$$\Delta i_{\mathrm{BCM}} = \overline{i_{L_{\mathrm{BCM}(1)}}} = \frac{1}{2}\hat{i}_{L_{\mathrm{BCM}(1)}} = \frac{\overline{i_{L_{\mathrm{CCM}}}}}{N} \tag{5}$$

where $\overline{i_{L_{\mathrm{BCM}(1)}}}$ is the average inductor current of a single phase of the N interleaved converters.

Using (4) and (5), the RMS current for CCM and each phase BCM operation can be calculated as

$$I_{\mathrm{RMS_{CCM}}} = \frac{\overline{i_{L_{\mathrm{CCM}}}}}{k}\,\frac{\sqrt{4k^2-2k+1}}{\sqrt{3}} \tag{6}$$

$$I_{\mathrm{RMS_{BCM(1)}}} = \frac{2}{\sqrt{3}}\Delta i_{\mathrm{BCM}} = \frac{2}{\sqrt{3}}\frac{\overline{i_{L_{\mathrm{CCM}}}}}{N}. \tag{7}$$

Initially assuming both cases operate the inductors at the same maximum field density $B_{\max}$, the single inductor A_p can, respectively, be calculated using (1) and (3)–(7) as

$$A_{p_{\mathrm{CCM}}} = \frac{L_{\mathrm{CCM}}\,\overline{i_{L_{\mathrm{CCM}}}}^2}{JB_{\max}K_w\sqrt{3}}\,\frac{\sqrt{4k^2-2k+1}}{k^2} \tag{8}$$

$$A_{p_{\mathrm{BCM}(1)}} = \frac{4L_{\mathrm{BCM}}}{JB_{\max}K_w\sqrt{3}}\,\frac{\overline{i_{L_{\mathrm{CCM}}}}^2}{N^2}. \tag{9}$$

Net volume ratio for 1-CCM and N-BCM converters is determined by combining (2), (8), and (9) as

$$\frac{\mathrm{Vol_{CCM}}}{\mathrm{Vol_{BCM}}_{(N)}} = \frac{(A_{p_{\mathrm{CCM}}})^{(3/4)}}{N(A_{p_{\mathrm{BCM}(1)}})^{(3/4)}} = \\ = \frac{1}{N}\left(\frac{L_{\mathrm{CCM}}}{L_{\mathrm{BCM}}}\,\frac{N^2\sqrt{4k^2-2k+1}}{4k^2}\right)^{(3/4)} \tag{10}$$

where $\mathrm{Vol}_{\mathrm{BCM}(N)}$ is the net N-BCM volume, corresponding to the N inductors for the N-phase interleaved converter.

From (10), volume ratio depends on inductance ratio $L_{\mathrm{CCM}}/L_{\mathrm{BCM}}$. As current ripple amplitude is inversely proportional to inductance value and switching frequency, and assuming the input and output voltages are the same in both cases, the inductance ratio using also (4) and (5) can be calculated as:

$$\frac{L_{\mathrm{CCM}}}{L_{\mathrm{BCM}}} = \frac{\Delta i_{\mathrm{BCM}}\,f_{sw_{\mathrm{BCM}}}}{\Delta i_{\mathrm{CCM}}\,f_{sw_{\mathrm{CCM}}}} = \frac{1}{f_R}\,\frac{k}{N(1-k)} \tag{11}$$

where $f_{sw_{\mathrm{CCM}}}$ and $f_{sw_{\mathrm{BCM}}}$ are the CCM and BCM switching frequencies, respectively, and $f_R = f_{sw_{\mathrm{CCM}}}/f_{sw_{\mathrm{BCM}}}$ is the frequency ratio.

Introducing (11) in (10), a new expression for volume ratio is obtained, as shown in (12). Noticing the switching frequency in BCM is inherently variable with the load current, calculations for BCM inductor are performed for the maximum power operating point, yielding the minimum switching frequency

$$\frac{\mathrm{Vol_{CCM}}}{\mathrm{Vol_{BCM}}_{(N)}} = \frac{1}{N^{1/4}}\left(\frac{1}{f_R}\,\frac{\sqrt{4k^2-2k+1}}{4k(1-k)}\right)^{(3/4)}. \tag{12}$$

From (12), volume ratio depends on N, the switching frequencies ratio, and the ripple factor k. This calculation, however, does not account for differences in core or winding losses. Therefore, in order to be able to compare volumes when inductor losses in the CCM and the N-BCM converters are similar, previous expression parameters should be modified.

Winding losses are a function of the length and cross sectional area of the conductor [14]. Therefore, these losses can be established by modifying the current density in each design. This is accomplished by defining $r_{J_{\mathrm{CCM}}}$ and $r_{J_{\mathrm{BCM}}}$ as the current density correction factors, i.e.,

$$J_{\mathrm{CCM}} = J \cdot r_{J_{\mathrm{CCM}}} \tag{13}$$

$$J_{\mathrm{BCM}} = J \cdot r_{J_{\mathrm{BCM}}}. \tag{14}$$

On the other hand, core loss is a function of the ac flux swing and the switching frequency, neglecting Foucault losses due to the low conductivity of the core material. In this condition, core losses can be estimated using methodologies based on the Steinmetz equation [15]. The improved generalized Steinmetz equation (iGSE) allows to accurately predict losses with arbitrary magnetic induction waveforms [16], [17]. Furthermore, i^2GSE has been presented in [18] in order to improve iGSE in applications where constant flux periods are present. Therefore, for CCM and BCM current waveforms where triangular excitation is present, iGSE is selected for the core power calculation, as shown below

$$P_{\mathrm{core}} = f_{sw}\int_0^{(1/f_{sw})} k_i \left|\frac{\mathrm{d}B}{\mathrm{d}t}\right|^{\alpha} (\Delta B)^{\beta-\alpha}\mathrm{d}t \cdot \mathrm{Vol} \tag{15}$$

where ΔB is the peak-to-peak flux density and k_i is defined as follows:

$$k_i = \frac{k_f}{(2\pi)^{\alpha-1}\int_0^{2\pi}|\cos\theta|^{\alpha}\,2^{\beta-\alpha}\mathrm{d}\theta}. \tag{16}$$

Parameters k_f, α, and β are the same parameters as the original Steinmetz equation, empirically obtained by experimental fitting. Particularly, k_f is a constant associated to the core material, exponent α is $1 \leq \alpha \leq 2$ and $2 \leq \beta \leq 3$.

For triangular excitation, and combining (15) with (16), the following expression for P_{core} is obtained:

$$P_{\text{core}} = C_m {f_{sw}}^{\alpha} \Delta B^{\beta} \text{Vol} \tag{17}$$

where C_m is a constant that depends on k_f, α, β and the duty cycle.

From previous expression, P_{core} is a function of ΔB. Therefore, this parameter will be used to equalize core losses in the CCM and the N-BCM designs, as usually core losses in BCM are larger than the CCM losses. Assuming the core is not driven into saturation, ΔB can be related to the number of turns n and to current ripple and peak values as [19]

$$\Delta B = \frac{L \Delta i}{n A_c} = \frac{L\ \Delta i\ I_{\text{RMS}}}{A_p\ J\ K_w} = B_{\max} \frac{\Delta i}{\hat{i_L}} \tag{18}$$

with the following replacement: $n = \frac{W_a J K_w}{I_{\text{RMS}}}$.

From (18), ΔB in BCM operation can be reduced by increasing n, which implies increasing W_a, and therefore A_p, in order to accommodate for the additional wire. Thus, if the number of turns is increased $r > 1$ times and the inductance is assumed to be restored to its initial value by increasing the air gap, ΔB is redefined as ΔB_r as shown in (19). It should be pointed out that this method is applicable whenever excessive gap length is not generated, as it could increment the winding losses. However, these losses can be greatly reduced by placing the wire windings away from the gap or distributing the total gap among the different core legs [20]

$$\Delta B_r = \frac{L \Delta i}{r\ n\ A_c} = B_{\max} \frac{\Delta i}{r\ \hat{i_L}} = \frac{\Delta B}{r}. \tag{19}$$

Therefore

$$\Delta B_{\text{CCM}} = B_{\max} \frac{\Delta i_{\text{CCM}}}{\hat{i_{L_{\text{CCM}}}}} = B_{\max}(1-k) \tag{20}$$

$$\Delta B_{\text{BCM}} = B_{\max} \frac{\Delta i_{\text{BCM}}}{r\ \hat{i_{L_{\text{BCM}}}}} = B_{\max} \frac{1}{2r}. \tag{21}$$

From (1), it can be seen that modifying the number of turns and the current density produce a variation in A_p. Therefore, so as to consider these redefined variables, a new A_p is defined for each design

$$A_{p_{\text{CCMr}}} = (1/r_{J_{\text{CCM}}}) A_{p_{\text{CCM}}} \tag{22}$$

$$A_{p_{\text{BCMr}}} = (r/r_{J_{\text{BCM}}}) A_{p_{\text{BCM}}}. \tag{23}$$

In order to obtain r, $r_{J_{\text{CCM}}}$, and $r_{J_{\text{BCM}}}$ values, core and winding losses are analyzed.

Winding losses are defined as $P_{Cu_{\text{CCM}}}$ and $P_{Cu_{\text{BCM}(1)}}$ for the CCM and a single BCM inductor, respectively. These losses are proportional to the current density squared [14]. Additionally, winding losses can be specified as a proportion of P_{core}, by using factors $r_{w_{\text{CCM}}}$ and $r_{w_{\text{BCM}}}$ for the CCM and the BCM cases, respectively

$$P_{Cu_{\text{CCM}}} = r_{w_{\text{CCM}}} P_{\text{core}_{\text{CCM}}}$$

$$\rho K_w \left(J \cdot r_{J_{\text{CCM}}}\right)^2 {A_{p_{CCM_r}}}^{(3/4)} = r_{w_{\text{CCM}}} P_{\text{core}_{\text{CCM}}} \tag{24}$$

$$P_{Cu_{\text{BCM}(1)}} = r_{w_{\text{BCM}}} P_{\text{core}_{\text{BCM}(1)}}$$

$$\rho K_w \left(J \cdot r_{J_{\text{BCM}}}\right)^2 {A_{p_{BCM_r}}}^{(3/4)} = r_{w_{\text{BCM}}} P_{\text{core}_{\text{BCM}(1)}} \tag{25}$$

where ρ is the copper resistivity. Then, combining previous expressions, the core losses ratio between the CCM and the N-BCM converter is obtained as

$$P_R = \frac{P_{\text{core}_{\text{CCM}}}}{P_{\text{core}_{\text{BCM}(N)}}} = \frac{P_{\text{core}_{\text{CCM}}}}{N P_{\text{core}_{\text{BCM}(1)}}}$$

$$= \frac{r_{w_{\text{BCM}}}}{N r_{w_{\text{CCM}}}} \left(\frac{r_{J_{\text{CCM}}}}{r_{J_{\text{BCM}}}}\right)^2 \left(\frac{A_{p_{\text{CCMr}}}}{A_{p_{\text{BCMr}}}}\right)^{3/4}. \tag{26}$$

Furthermore, from (17) and assuming BCM and CCM magnetic parts use the same core material, and that temperature, input and output voltages are also the same, the core power losses for both operation modes can be calculated per

$$P_{\text{core}_{\text{CCM}}} = C_m {f_{sw_{\text{CCM}}}}^{\alpha} B_{\max}^{\beta} (1-k)^{\beta} {A_{p_{\text{CCMr}}}}^{(3/4)} \tag{27}$$

$$P_{\text{core}_{\text{BCM}(N)}} = N \left[C_m {f_{sw_{\text{BCM}}}}^{\alpha} \frac{B_{\max}^{\beta}}{(2r)^{\beta}} {A_{p_{\text{BCMr}}}}^{(3/4)} \right]. \tag{28}$$

Consequently, combining expressions from (24) to (28), the value of r can be calculated for a given P_R and winding to core losses ratio as

$$r = \left(\frac{{P_R}^{8/5}}{{f_R}^{\alpha} (2(1-k))^{\beta} \left(\frac{\text{Vol}_{\text{CCM}}}{\text{Vol}_{\text{BCM}(N)}}\right)^{8/5} \left(\frac{r_{w_{\text{BCM}}}}{r_{w_{\text{CCM}}}}\right)^{3/5}} \right)^{\frac{1}{\beta - 6/5}}. \tag{29}$$

Finally, Vol_R is defined as the volume ratio for a given core losses ratio P_R, and considering that losses in the winding are $r_{w_{\text{CCM}}}$ and $r_{w_{\text{BCM}}}$ relative to the CCM and BCM core losses, respectively. Combining (29), (26), and (12), Vol_R is obtained as

$$\text{Vol}_R = \frac{\text{Vol}_{\text{CCM}}}{\text{Vol}_{\text{BCM}(N)}} \left(\frac{r_{J_{\text{CCM}}}}{r r_{J_{\text{BCM}}}}\right)^{3/4} =$$

$$\text{Vol}_R = \left(\frac{\sqrt{4k^2 - 2k + 1}}{2k} \right)^{\left(\frac{6\beta}{5\beta - 6}\right)} N^{\left(\frac{2\beta}{6-5\beta}\right)} P_R^{\left(3\frac{(\beta+2)}{6-5\beta}\right)}$$

$$\cdot\ {f_R}^{\left(\frac{6(\alpha-\beta)}{5\beta-6}\right)} \left(\frac{r_{w_{\text{BCM}}}}{r_{w_{\text{CCM}}}}\right)^{3\beta/(5\beta-6)}. \tag{30}$$

Expression (30) can be analyzed to obtain the CCM-to-BCM volume ratio dependence with N, f_R, P_R, and k. Considering $2 \leq \beta \leq 3$ and $1 \leq \alpha \leq 2$, it can be concluded that:

1) as Vol_R is proportional to $N^{\left(\frac{2\beta}{6-5\beta}\right)}$, the volume ratio increases when N decreases;
2) Vol_R decreases when P_R is increased, as allowing more losses in one mode (BCM or CCM), a volume reduction is obtained in that same mode compared to the other;

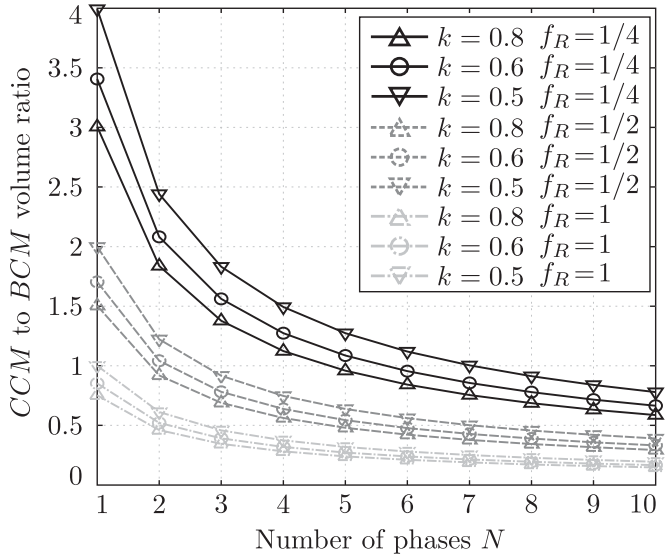

Fig. 2. Volume ratio as a function of N, $P_R = 1$ and $r_{w_{\mathrm{CCM}}} = r_{w_{\mathrm{BCM}}} = 1$.

3) Vol_R increases when k is decreased, i.e., as CCM ripple is being increased, approaching the BCM behavior;
4) Vol_R increases when f_R decreases ($f_{sw_{\mathrm{BCM}}}$ higher than $f_{sw_{\mathrm{CCM}}}$). As BCM converters operate with lower switching losses in the semiconductors, it becomes possible to run the converters at $f_{sw_{\mathrm{BCM}}} > f_{sw_{\mathrm{CCM}}}$.

The implications of the analysis performed can be illustrated by taking typical values. For switching frequencies between 20 and 200 kHz we can assume $\alpha = 1.46$ and $\beta = 2.75$ [21]. Fig. 2 shows the volume ratio as a function of N, calculated using (30) for different values of k and f_R, assuming the same core losses on both operating modes, i.e., $P_R = 1$, and that the cores and winding losses are the same, i.e., $r_{w_{\mathrm{CCM}}} = r_{w_{\mathrm{BCM}}} = 1$. k values 0.5, 0.6, and 0.8 correspond to CCM ripple values 50 %, 40 %, and 20 % of peak current, respectively.

As it can be seen, for a given $f_R = f_{sw_{\mathrm{CCM}}}/f_{sw_{\mathrm{BCM}}}$ and k, CCM-to-N-BCM volume ratio decreases when N increases. Additionally, it can be noticed that volume ratio decreases when k is increased, as previously discussed. On the other hand, increasing BCM switching frequency, which is possible due to the reduced losses on the switches, leads to a volume reduction. For example, using $k = 0.8$ and $f_R = 1/2$, CCM and 2-phase BCM, yields approximate the same volume, while if N is increased to 5, 5-BCM occupies twice the volume than single phase CCM.

A. Practical Case Analysis

In order validate the proposed methodology, the input inductors for both, a single phase CCM as well as for an N-phase BCM boost converters are calculated. The volume ratio obtained by design is compared to the volume ratio predicted by (30) to verify its accuracy. The design specifications for the converter are summarized in Table I.

From the parameters listed in Table I, and assuming the efficiency is close enough to 1, total input average current results

$$\overline{i_{L_{\mathrm{CCM}}}} = \frac{P_o}{V_{\mathrm{in}}}. \tag{31}$$

TABLE I
DESIGN SPECIFICATIONS

Parameter	Value
Output power, P_o	1000 W
Input RMS voltage, V_{in}	220 V
Output voltage, V_o	400 V
Max. current density, J	4 A/mm^2
Maximum field density, B_{max}	0.35 T
Copper fill factor, K_w	0.6

TABLE II
CCM AND N-BCM INDUCTOR PARAMETERS

Mode	Δi	L value	ΔB	A_p
CCM	1.6 A	308 μH	138.2 mT	3842 mm^4
1-BCM	6.43 A	39 μH	109.87 mT	2314 mm^4
2-BCM	3.21 A	77 μH	92.8 mT	1706 mm^4
3-BCM	2.14 A	116 μH	83.3 mT	1476 mm^4
4-BCM	1.61 A	154 μH	77.6 mT	1304 mm^4
5-BCM	1.29 A	193 μH	73.11 mT	1205 mm^4
6-BCM	1.07 A	231 μH	69.89 mT	1115 mm^4
7-BCM	0.92 A	270 μH	67.07 mT	1056 mm^4
8-BCM	0.8 A	308 μH	64.89 mT	997 mm^4
9-BCM	0.71 A	347 μH	62.88 mT	957 mm^4
10-BCM	0.64 A	385 μH	61.26 mT	915 mm^4

TABLE III
CCM AND N-BCM INDUCTORS

Mode	Core	$A_{p_{\mathrm{core}}}$	Volume	n	Gap length
CCM	E25/13/11	4282 mm^4	4500 mm^3	91	2.62 mm
1-BCM	E25/13/7	2910 mm^4	2990 mm^3	28	1.292 mm
2-BCM	E25/10/6	2220 mm^4	1930 mm^3	36	0.831 mm
3-BCM	E25/10/6	2220 mm^4	1930 mm^3	36	0.554 mm
4-BCM	E25/10/6	2220 mm^4	1930 mm^3	36	0.415 mm
5-BCM	E25/10/6	2220 mm^4	1930 mm^3	36	0.332 mm
6-BCM	E20/10/6	1120 mm^4	1490 mm^3	45	0.346 mm
7-BCM	E20/10/6	1120 mm^4	1490 mm^3	45	0.297 mm
8-BCM	E20/10/6	1120 mm^4	1490 mm^3	45	0.26 mm
9-BCM	E20/10/6	1120 mm^4	1490 mm^3	45	0.231 mm
10-BCM	E20/10/6	1120 mm^4	1490 mm^3	45	0.208 mm

Expressions from (3) to (7) help in computing the inductor values and the parameters required for the area product calculation. For this example, CCM ripple factor is set to $k = 0.8$ and CCM switching frequency to $f_{sw_{\mathrm{CCM}}} = 100$ kHz. On the other hand, BCM switching frequency is set to $f_{sw_{\mathrm{BCM}}} = 2f_{sw_{\mathrm{CCM}}} = 200$ kHz. Table II summarizes the inductors values, the current ripple amplitude, the ac flux density, and the calculated area-product for each design.

The inductors obtained using the standard design procedure described in [19] are shown in Table III. In all the cases Ferroxcube's 3C94 ferrite E-cores have been used, whose Steinmetz parameters are $k_f = 2.37 \cdot 10^{-3}$, $\alpha = 1.46$, and $\beta = 2.75$ for the frequency range from 20 to 200 kHz. Selected magnetic cores have the nearest larger area product for each case. It should be noted that, as commercial E cores have limited size and shapes, not all product areas are available and some discrepancies have to be expected.

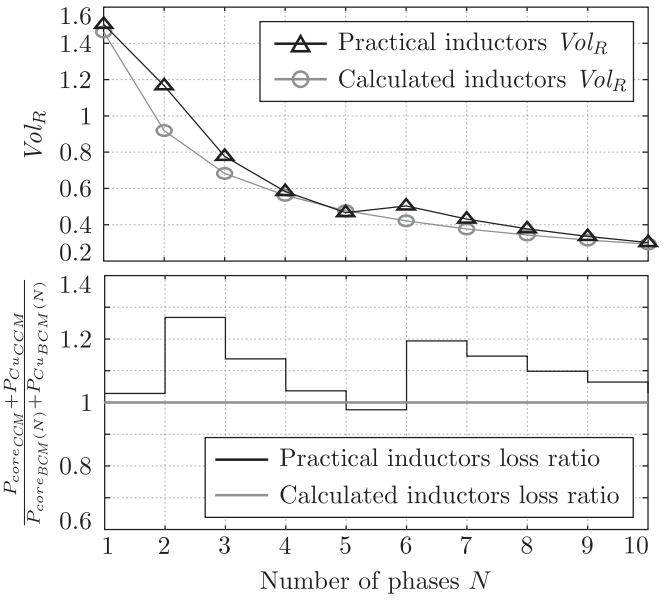

Fig. 3. Volume and power losses ratios of practical inductors design.

Fig. 3 shows the volume ratio and total (core and winding) power losses ratio for the above presented designs. Power losses ratio, which is expected to be equal to 1 by the constraints imposed for the calculations, is obtained by computing the core dissipation of each core using the calculated ΔB, listed in Table II, and the core manufacturer curves, while winding losses are calculated by using the procedure described on [14]. As it can be seen, real Vol_R follows the volume ratio predicted by (30) in the average. Discrepancies in the practical inductor calculations are due to discrete availability in core size.

III. Conclusion

In this paper, a method for estimating the inductor volume ratio between a single CCM and N-phase interleaved BCM power converters has been presented. Volumes for each operating mode have been calculated using the area product definition and taking into consideration the core and winding power losses. As a result, a closed expression for the volume ratio has been found including design parameters, such as the number of BCM phases, CCM peak-to-average current ratio, core-to-winding losses ratio, as well as inductor power loss ratio and switching frequency ratio between the CCM and BCM designs. The presented method is, therefore, a useful tool that can be used in combination with efficiency calculations, already available in the literature, to determine the optimal number of phases for a given application. The proposed method can be applied to boost, flyback, and forward topologies. In the boost case, the inductor current is the input current, while in the forward case its inductor current becomes the converter output current. On the other hand, in the flyback case, there would be no direct relationship to either input or output current, but through the introduction of the duty cycle. One extra advantage of the interleaved topology not included in this analysis, is the increased dissipation surface on the magnetic parts for the same volume, which would provide an extra advantage on N-BCM topologies over 1-CCM ones.

References

[1] Y.-S. Kim, W.-Y. Sung, and B.-K. Lee, "Comparative performance analysis of high density and efficiency PFC topologies," *IEEE Trans. Power Electron.*, vol. 29, no. 6, pp. 2666–2679, Jun. 2014.

[2] O. Hegazy, J. V. Mierlo, and P. Lataire, "Analysis, modeling, and implementation of a multidevice interleaved DC/DC converter for fuel cell hybrid electric vehicles," *IEEE Trans. Power Electron.*, vol. 27, no. 11, pp. 4445–4458, Nov. 2012.

[3] X. Xu, W. Liu, and A. Q. Huang, "Two-phase interleaved critical mode PFC boost converter with closed loop interleaving strategy," *IEEE Trans. Power Electron.*, vol. 24, no. 12, pp. 3003–3013, Dec. 2009.

[4] H. Choi and L. Balogh, "A cross-coupled master-slave interleaving method for boundary conduction mode (BCM) PFC converters," *IEEE Trans. Power Electron.*, vol. 27, no. 10, pp. 4202–4211, Oct. 2012.

[5] P. D. Antoszczuk, R. G. Retegui, N. Wassinger, S. Maestri, M. Funes, and M. Benedetti, "Characterization of steady-state current ripple in interleaved power converters under inductance mismatches," *IEEE Trans. Power Electron.*, vol. 29, no. 4, pp. 1840–1849, Apr. 2014.

[6] K. Raggl, T. Nussbaumer, G. Doerig, J. Biela, and J. Kolar, "Comprehensive design and optimization of a high-power-density single-phase boost PFC," *IEEE Trans. Ind. Electron.*, vol. 56, no. 7, pp. 2574–2587, Jul. 2009.

[7] P. Antoszczuk, R. Retegui, M. Funes, N. Wassinger, and S. Maestri, "Interleaved current control for multiphase converters with high dynamics mean current tracking," *IEEE Trans. Power Electron.*, to be published.

[8] J. Shen, K. Rigbers, and R. W. De Doncker, "A novel phase-interleaving algorithm for multiterminal systems," *IEEE Trans. Power Electron.*, vol. 25, no. 3, pp. 741–750, Mar. 2010.

[9] O. García, P. Zumel, A. de Castro, and J. A. Cobos, "Automotive dc-dc bidirectional converter made with many interleaved buck stages," *IEEE Trans. Power Electron.*, vol. 21, no. 3, pp. 578–586, May 2006.

[10] S. M. Ahsanuzzaman, A. Prodic, and D. A. Johns, "An integrated high-density power management solution for portable applications based on a multioutput switched-capacitor circuit," *IEEE Trans. Power Electron.*, vol. 31, no. 6, pp. 4305–4323, Jun. 2016.

[11] M. S. Perdigao, J. P. F. Trovao, J. M. Alonso, and E. S. Saraiva, "Large-signal characterization of power inductors in EV bidirectional dc-dc converters focused on core size optimization," *IEEE Trans. Ind. Electron.*, vol. 62, no. 5, pp. 3042–3051, May 2015.

[12] L. Gu, J. Sun, M. Xu, Q. Zuo, and J. Fan, "Size reduction of the inductor in critical conduction mode PFC converter," in *Proc. IEEE 26th Annu. Appl. Power Electron. Conf. Expo.*, Mar. 2011, pp. 550–557.

[13] W. G. Hurley and W. H. Wölfle, *Transformers and Inductors for Power Electronics: Theory, Design and Applications*. New York, NY, USA: Wiley, 2013.

[14] W.-J. Gu and R. Liu, "A study of volume and weight vs. frequency for high-frequency transformers," in *Proc. IEEE Power Electron. Spec. Conf.*, 1993, pp. 1123–1129.

[15] J. Reinert, A. Brockmeyer, and R. De Doncker, "Calculation of losses in ferro- and ferrimagnetic materials based on the modified Steinmetz equation," *IEEE Trans. Ind. Appl.*, vol. 37, no. 4, pp. 1055–1061, Jul./Aug. 2001.

[16] K. Venkatachalam, C. Sullivan, T. Abdallah, and H. Tacca, "Accurate prediction of ferrite core loss with nonsinusoidal waveforms using only Steinmetz parameters," in *Proc. IEEE Workshop Comput. Power Electron.*, 2002, pp. 36–41.

[17] Jieli Li, T. Abdallah, and C. Sullivan, "Improved calculation of core loss with nonsinusoidal waveforms," in *Proc. IEEE Ind. Appl. Soc. Annu. Meeting*, 2001, pp. 2203–2210.

[18] J. Mühlethaler, J. Biela, J. W. Kolar, and A. Ecklebe, "Core losses under the DC bias condition based on Steinmetz parameters," *IEEE Trans. Power Electron.*, vol. 27, no. 2, pp. 953–963, Feb. 2012.

[19] R. W. Erickson and D. Maksimovic, *Fundamentals of Power Electronics*. Berlin, Germany: Springer Science & Business Media, 2007.

[20] R. Jensen and C. Sullivan, "Optimal core dimensional ratios for minimizing winding loss in high-frequency gapped-inductor windings," in *Proc. IEEE 18th Annu. Appl. Power Electron. Conf. Expo.*, 2003, pp. 1164–1169.

[21] R. R. E. Ridley and A. Nace, "Modeling ferrite core losses," *Switch. Power Mag.*, pp. 8–9, 2006.